

Improved Fourier Based Method for Calculating Field Inhomogeneity from Known Susceptibility Distribution

J. Neelavalli¹, Y. Norman Cheng², and E. M. Haacke²

¹Biomedical Engineering, Wayne State University, Detroit, MI, United States, ²Wayne State University, MI, United States

Introduction: Static field inhomogeneities due to magnetic susceptibility differences between adjacent tissues or at air-tissue interfaces lead to signal loss in images, and degrade the quality of MR spectroscopy data. Hence quantifying the susceptibility effects is important for correcting for these effects as well as for various applications like geometric distortion correction, modeling effects of respiration on MR signal in fMRI, and better 3D shimming [1-5]. Several research groups have investigated a fast, Fourier Transform based method for magnetic field calculations [2,5,6], that utilizes the fact that the expression for the magnetic field deviation $B_d(\mathbf{r})$ at a location \mathbf{r} , due to a source magnetization distribution $\mathbf{M}(\mathbf{r}')$, is a convolution of the Green's function and the magnetization.

The magnetization of any non ferric material is proportional to the susceptibility at a given location i.e., $\mathbf{Mz}(\mathbf{r}') \approx \chi(\mathbf{r}') * \mathbf{B}_0 / \mu_0$ (assuming B_0 is along z direction). When the object size is small compared to the size of the field of view (FOV), the previous work in the literature has shown that the calculated field distribution based on an analytical solution agrees well with theoretical solutions. However, when the object size increases, the calculated field distribution deviates considerably from the theoretical values. In an attempt to reduce the error in the calculated field maps, we present here an improved modification of the method. We demonstrate the success of our method by considering the field distribution due to a sphere, which has a susceptibility difference inside and outside the sphere.

Theory and Methods: In the case of MR imaging, we are only interest in the field component parallel to the main field strength, B_0 . The z-component of the magnetic field distribution $B_{dz}(\mathbf{r})$ at a point \mathbf{r} due to a susceptibility distribution $\chi(\mathbf{r}')$ is given by Eq(1) where $G_z(\mathbf{r}-\mathbf{r}')$ is the Green's function given by Eq(2):

$$B_{dz}(\mathbf{r}) = \int_{V'} M_z(\mathbf{r}') G_z(\mathbf{r}-\mathbf{r}') dV' \dots \dots eq(1);$$

$$G_z(\mathbf{r}-\mathbf{r}') = \frac{\mu_0}{4\pi} * \left\{ \frac{3(z-z')^2}{|\mathbf{r}-\mathbf{r}'|^5} - \frac{1}{|\mathbf{r}-\mathbf{r}'|^3} \right\} \dots \dots eq(2);$$

$$B_{dz}(\mathbf{r}) = B_0 * FT^{-1} [G_d(k) * FT(\chi(r))] \dots \dots eq(3);$$

$$G_d(k) = FT(G_z(\mathbf{r})) \dots \dots eq(4);$$

$$B_{dz}(\mathbf{r}) = B_0 * FT^{-1} \left[\left[\frac{1}{3} \frac{k_z^2}{k_x^2 + k_y^2 + k_z^2} \right] * FT(\chi(r)) \right] \dots \dots (5)$$

After applying the Fourier transformation (FT) and inverse Fourier transformation on both sides of Eq(1) and with Eq(2) as well as Fourier convolution theorem, Eq(1) can be rewritten as Eq(3). Thus, the algorithm for calculating field map is 1) Fourier transforming the susceptibility (χ) matrix, 2) multiplying the $FT[\chi(\mathbf{r})]$ with the Green's function in the k-space domain, and 3) taking the inverse-FT of the product of the two functions.

When the field of view is infinite, Eq(5) can be analytically derived. Its result lead Eq(1) to Eq(5) with $G_c(k) \equiv \mu_0 [1/3 - kz^2/(kx^2+ky^2+kz^2)]$. However, when the field of view is finite, the Green's function in the k-space domain $G_d(k) = FT[\mu_0 (2z^2-x^2-y^2) / 4\pi (x^2+y^2+z^2)^{5/2}]$ from eq (3) has to be numerically calculated. We will show below that such a correction between $G_d(k)$ and $G_c(k)$ is significant. To evaluate the results from both $G_d(k)$ and $G_c(k)$, we simulate a series of field distributions based on spheres of radii 8, 16, 32, and 48 pixels in a finite size 3D matrix of dimensions 128x128x128 pixels. In all the simulations, a susceptibility value of -9 ppm was assigned to the sphere and a value of 0 was assigned to the region outside the sphere. In each case we simulate two field maps, one using $G_c(k)$ and the other one using $G_d(k)$. We compare results generated from $G_c(k)$ and $G_d(k)$ as well as the theoretical field map.

Results: To quantify the error distribution over the entire 3D volume and also to see the effect of increasing object size on the error, the values corresponding to 90th and the 99th percentile pixels are calculated for different radii in Table 1. The percentile values are to be interpreted as: 90% or 99% of the pixels within the entire 3D field of view has an absolute error less than the specified ppm value in the table. Table 1 shows that the errors are dramatically reduced with this new k-space filter function $G_d(k)$. Specifically, for $R = 8$ and 16, the errors are reduced by nearly a factor of 10. To show this more clearly, we plot the error as a function of position for $R=32$ (Fig 1b), $R=8$ (Fig. 1c) and $R=16$ (Fig.1d). Since the field itself in the center of the sphere is zero, the percentage error cannot be calculated inside the sphere and hence those values are absent in the plots. Clearly, from Fig 1, the field predicted when $G_d(k)$ is used, is closer to the theoretical value than that from $G_c(k)$. Figure 2 maps the absolute field errors in a plane with the sphere of radius 32 pixels with 2a and 2b corresponding to results from using $G_c(k)$ and $G_d(k)$, respectively. In order to ignore the large errors due to ghosting artifacts at the boundary of the spheres, and better visualize the error distributions outside the spheres, the gray scales in image are adjusted between 0 to 20% of the maximum absolute theoretical field (i.e., 1.2 ppm in this case).

Discussion: In general, the Fourier method suffers errors from mainly two factors: discretization and finite field of view. The former has not been studied yet. The latter introduces two types of errors. First, because of finite field of view and calculations of Fourier transformations, the calculated field distributions becomes a result from periodically repeated susceptibility sources rather than one susceptibility source. This fact leads to large errors at the edges of the field of view, unless the source object becomes small compared to the field of view [2, 7]. This type of error decreases when the object size decreases with respect to the field of view, as shown in fig 1c and d, and in the Table 1. Second, the significant ghosting artifact at the edges of the spheres is also due to the finite field of view, which will not be removed. In summary, we have demonstrated that the Green's function generated from the discretized Fourier transformation significantly reduces the error in the Fourier based method of calculating the magnetic field due to susceptibility distributions.

References: (1) Jenkinson M. et al MRM:52:471 (2)Marques J.P. et al Conc. Magn. Reson. B:25:65 (3)Raj D et al Phys. Med. Biol. 45:3809 (4) Jezzard P et al., MRM:34:65 (5)Koch et al Proc ISMRM-06,Seattle p518 (6) R. Salomir, et al Concepts Magn. Reson B., 19B, 26-34 (7)Ledbetter M.P. et al J Chem. Phys. 121:3:1454.

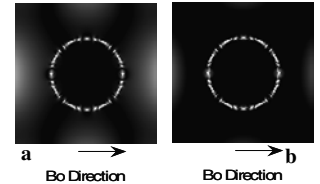


Fig 2 a ,b. Absolute Field error maps

Maximum absolute Field deviation=5.9 9ppm	Field error corresponding to Gc(k)		Field error corresponding to Gd(k)	
	90 th in ppm	99 th in ppm	90 th in ppm	99 th in ppm
Radius R=8	0.0034	0.0069	0.00042	0.0037
R=16	0.0261	0.056	0.00261	0.016
R=32	0.2153	0.454	0.063	0.25
R=48	0.719	1.38	0.37	0.96

Table 1

